

## CMAS: fully integrated portable centrifugal microfluidic analysis system for on-site colorimetric analysis†

Cite this: DOI: 10.1039/c3ra42975j

Monika Czugała,<sup>a</sup> Damian Maher,<sup>a</sup> Fiachra Collins,<sup>a</sup> Robert Burger,<sup>b</sup> Frank Hopfgartner,<sup>a</sup> Yang Yang,<sup>a</sup> Jiang Zhaou,<sup>a</sup> Jens Ducreé,<sup>b</sup> Alan Smeaton,<sup>a</sup> Kevin J. Fraser,<sup>\*a</sup> Fernando Benito-Lopez<sup>\*ac</sup> and Dermot Diamond<sup>a</sup>

A portable, wireless system capable of *in situ* reagent-based colorimetric analysis is demonstrated. The system is based on a reconfigurable low cost optical detection method employing a paired emitter detector diode device, which allows a wide range of centrifugal microfluidic layouts to be implemented. Due to the wireless communication, acquisition parameters can be controlled remotely and results can be downloaded in distant locations and displayed in real time. The stand-alone capabilities of the system, combined with the portability and wireless communication, provide the flexibility crucial for on-site water monitoring. The centrifugal microfluidic disc presented here is designed for nitrite detection in water samples, as a proof of principle. A limit of detection of 9.31 ppb, along with similar coefficients of correlation and precision, were obtained from the Centrifugal Microfluidic Analysis System compared with the same parameters measured using a UV-Vis spectrophotometer.

Received 14th June 2013,  
Accepted 4th July 2013

DOI: 10.1039/c3ra42975j

[www.rsc.org/advances](http://www.rsc.org/advances)

### Introduction

Currently, water quality monitoring is still largely based on manual sample collection and subsequent laboratory testing, despite the very costly and time-consuming nature of this approach. Therefore the development of fast, accurate and robust *in situ* monitoring techniques, which can provide the required analytical information at a much lower cost, would be of great benefit.<sup>1</sup> The availability of easy to use and low cost analytical measurements is the key to future scalability in terms of the number of locations that can be sampled and the sampling frequency, thus facilitating the emergence of higher resolution temporal and spatial monitoring strategies.

There is a wide range of commercially available portable devices that can provide rapid indication of water quality parameters. Some techniques are relatively cheap (<100 USD), but they do not possess data logging capabilities and allow for only one spot test (e.g. Hanna instruments nitrite ULR Checker (HI 764),<sup>2</sup> and API<sup>®</sup> test kits).<sup>3</sup> Conversely, more sophisticated probes allow multi-parameter measurements with integrated wireless data transmission, but their application is quite limited due to the high cost of hardware and maintenance

(Hach<sup>®</sup> Hydrolab DS5<sup>4</sup> and YSI<sup>®</sup> V2 Multiparameter Water Quality Sondes,<sup>5</sup> costs typically \$20 K USD or greater).

Micro total analysis systems ( $\mu$ TAS) provide a route for the generation of micro-dimensioned analytical instruments that can be operated in remote locations, enabling *in situ* water analysis to become a reality.<sup>6</sup> It has been previously described that there are clear advantages of using microfluidic devices in the integration of sample processing in order to meet the increasing needs of modern environmental monitoring.<sup>7</sup> The small amounts of sample and reagents typically required, the ability to generate results rapidly and the use of a single motor to control complex fluidic transport make “lab-on-a-disc” based platforms attractive options for generating fully integrated  $\mu$ TAS platforms.<sup>8,9</sup> Several implementations of centrifugal discs for environmental monitoring have been reported;<sup>10</sup> Salin *et al.* developed discs for the detection of aqueous sulfide,<sup>11</sup> nitrate, nitrite<sup>12</sup> and chromium VI<sup>10</sup> employing centrifugal microanalysis. More recently, Hwang *et al.*<sup>13</sup> published a microfluidic centrifugal disc that is capable of simultaneous determination of several nutrients in water samples (nitrite, nitrate, ammonium, orthophosphate, and silicate). However, in these cases a bench-top fiber-based optics/spectrophotometer system was employed for the optical detection.<sup>11,13</sup> Therefore, while these platforms did demonstrate the excellent use of centrifugal discs for implementing environmental assays, the devices were not suitable for *in situ* remote water quality monitoring.

While many individual analysis steps and functions for centrifugal discs have been demonstrated, there are relatively few examples of fully integrated sample-to-answer centrifugal

<sup>a</sup>CLARITY: Centre for Sensor Web Technology, National Centre for Sensor Research, Dublin City University, Dublin, Ireland. E-mail: cyrusmekon@gmail.com; fbenito@cicmicrogune.es

<sup>b</sup>Biomedical Diagnostics Institute, National Centre for Sensor Research, Dublin City University, Dublin, Ireland

<sup>c</sup>CIC microGUNE, Arrasate-Mondragón, Spain

† Electronic supplementary information (ESI) available. See DOI: 10.1039/c3ra42975j

systems for environmental analysis. One challenge to overcome is the complex and expensive hardware platform required for complete analysis<sup>8</sup> where motor control, analysis instrumentation, optical systems and other equipment must be integrated in a cost effective way. In centrifugal microfluidics, optical detection remains the preferred technique for quantitative analysis as CD platforms are manufactured with high optical quality plastics that enable absorbance and fluorescence to be employed. Due to the rapid reduction in the cost of quality optoelectronic components like laser diodes, photodiodes, CCD cameras and light emitting diodes (LEDs), optical detection is becoming more practical for point-of-care (POC) diagnostics. Specifically, the advancement in LED sources and photodetector technologies provides a solution to all these issues. In particular, due to their small size, low cost, increasing spectral range coverage (247–1550 nm), low power consumption, efficiency and ease of fabrication, paired emitter detector diode (PEDD) based systems provide an excellent solution to the incorporation of colorimetric and fluorescence analytical detection into remotely deployable devices.<sup>6,14</sup>

Despite the advances described above, few successful integrated systems employ centrifugal discs. Several of these integrated systems have been published for point-of-care biomedical diagnostics<sup>15,16</sup> applications and only a few functioning systems are available in the market. For instance, the Piccolo clinical blood analyser system from Abaxis can process whole blood samples, and is one of the first examples of a disc-based sample-to-answer systems.<sup>16</sup> The colorimetric absorbance measurements are performed using an off-disc spectrophotometer. In addition, calibration is carried out simultaneously as the reference solutions are read from the disc reference cuvettes. Ducreé *et al.*<sup>17,18</sup> have also shown the successful integration of blood-plasma separation and colorimetric-based analyte detection systems.<sup>17,18</sup> They demonstrated a bench-top device for a fully integrated processing and read-out of the hemoglobin assay, which comprises a PC-controlled actuation unit, a synchronised free-droplet dispenser unit to load the reagents, a low-cost laser and a spectrophotometer as components for the optical detection. The use of a spectrophotometer ensures a flexible read-out of additional colorimetric assays or even fluorescence immunoassays (FIA),<sup>19</sup> allowing different types of assays to be run on the same disc, either simultaneously or sequentially. Also techniques for on-board-storage and release of liquid reagents have been successfully integrated in the meantime.<sup>20,21</sup>

The nitrite ion is ubiquitous within environmental, industrial, food and physiological systems.<sup>22</sup> Excessive levels can lead to detrimental human health effects and marine life degradation.<sup>23,24</sup> Current techniques for the detection of nitrite are electrochemical, capillary/column, biosensing, however spectrophotometric methods are the most popular by far,<sup>22</sup> due to the excellent limits of detection (as low as sub-nanomolar), dynamic range and cost efficiency. In particular, the spectrophotometric assay based on the Griess reagent has been very popular for over a century.<sup>23</sup> This assay is well-

known for its sensitivity, stability and robustness, but existing flow injection analysis systems tend to consume large volumes of reagent (mL per sample),<sup>25</sup> and are thus unsuitable for *in situ* and remote deployment. Recently Xi *et al.*<sup>26</sup> determined nitrite/nitrate concentrations in water samples using the Griess reagent method on a centrifugal microfluidic disc. The authors concluded that use of powdered reagents was compatible with the centrifugal disc format and suitable for field use.

Currently, commercially available systems for water analysis have limited on site usage capabilities, mainly due to their large size,<sup>27</sup> high power consumption (typically 10–150 W),<sup>28</sup> and excessive reagent usage (mL per sample).<sup>27</sup> Therefore a stand-alone, compact and low power environmental sensor that requires minimal reagent could have significant impact. In this report, we present the design and the development of a fully integrated portable centrifugal microfluidic analysis system (CMAS) for on-site lab-on-a-disc colorimetric analysis. CMAS is coupled *via* Bluetooth to an Android tablet for data collection, geotagging and Cloud sharing. Unlike the first generation system,<sup>29</sup> CMAS employs not only colorimetric chemical detection, but also centrifugal disc spinning, enabling on site sample manipulation analysis. CMAS has a modular design with easily interchangeable optical detection units, which allow any colorimetric reagent based assay to be implemented. As a proof of concept, the analysis of nitrite from environmental water samples is carried out in the system and compared to results obtained with a standard bench-instrument.

## Experimental

### Chemicals and reagents

All solutions were prepared from analytical grade chemicals and deionised water from a Millipore Milli-Q Q-GARD<sup>®</sup> 1 water purification system. Stock solutions were prepared freshly prior use and stored in dark environment at room temperature for no longer than one week. The Griess reagent was prepared following previously published procedures.<sup>30</sup> Phosphoric acid (H<sub>3</sub>PO<sub>4</sub>), sulfanilic acid, *N*-(1-naphthyl)ethylenediamine dihydrochloride (NED) and sodium nitrite (NaNO<sub>2</sub>) were purchased from Sigma-Aldrich<sup>®</sup>, Ireland and used without further purification. Nitrite standard solutions were diluted from a 200 mg L<sup>-1</sup> NaNO<sub>2</sub> stock solution to the appropriate concentrations.

### Centrifugal microfluidic fabrication

The centrifugal disc presented here consists of a multi-layer structure made of poly(methyl methacrylate) (PMMA) plastic and double-sided, pressure-sensitive adhesive (PSA). Using a CO<sub>2</sub> laser ablation system (Epilog Zing Laser Engraver, USA) fluid reservoirs were machined into 1.5 mm PMMA plastic (Radionics, Ireland). A cutter-plotter (Graphtec, Japan-Graphtec) was used to cut channels of 1 mm width in an 86 μm thick pressure sensitive adhesive layer (PSA, AR8890, Adhesives Research, Ireland). Once the appropriate pieces had

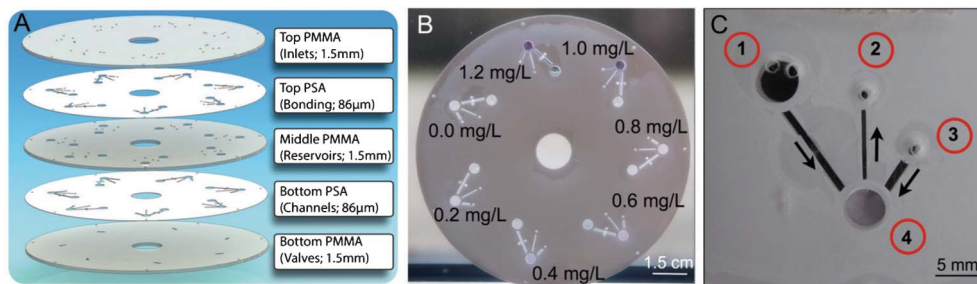


**Fig. 1** (A) Schematic showing the assembly of the centrifugal disc, (B) fully assembled centrifugal disc for determination of nitrite with seven microfluidic structures filled with different concentrations of nitrite and (C) image showing the detailed microfluidic layout and functions: 1–inlet for sample, 2–air vent, 3–inlet for the reagent, 4–mixing/detection chamber.

been designed and machined, they were aligned centrally as well as azimuthally and bonded using the PSA layers. The CD consists of 5 layers: (1) top PMMA disc with laser-machined sample and reagent loadings and air venting hole, (2) pressure-sensitive adhesive with reservoirs features cut using a plotter, (3) middle PMMA disc with sample and reagent reservoirs (radius 2.25 mm and 0.5 mm, respectively), and detection chamber (radius 2.2 mm), (4) pressure-sensitive adhesive with microchannel features cut using a plotter, (5) solid PMMA disc to seal off the channels (Fig. 1a). When assembled, the centrifugal disc allows complex 3D fluidics through the use of multiple layers. Fig. 1b shows a fully assembled CD for the determination of nitrite consisting of seven microfluidic structures and the detailed microfluidic layout and functions, Fig. 1c.

### Instrumentation

**CMAS hardware.** CMAS incorporates wireless communication and is powered *via* two 9 V lithium polymer batteries. A Pololu Wixel-based general-purpose programmable module based on a TI CC2511F32 microcontroller controls the entire system operation. System control and data acquisition are wirelessly enabled in real time by the use of Bluetooth communication (BlueSMiRF RN-42) with a custom designed interface on an Android tablet. A pulse-width modulation (PWM) controlled motor (Mabuchi Motor RF-500TB) enables spinning of the disc, thus allowing for the loading of the samples to the detection chambers. CD speed is calculated using an optical switch (Optek OPB830L51) and rotating interrupter.

The in-house designed CMAS case was fabricated using a 3D printer (Stratasys, USA) in acetonitrile butadiene styrene copolymer (ABS) plastic in order to protect the electronics and to minimise interferences from ambient light during the operation of the device. The printed parts were designed using ProEngineer CAD/CAM software package, 3D rendered pictures are presented below. Fig. S1A, ESI† presents a schematic of the bottom side of CMAS, wherein the two batteries, motor and the other electronic components are integrated. In Fig. S1B, ESI† the side view of the CMAS with loaded centrifugal disc is shown, whereas Fig. S1C, ESI† presents an exploded view of the system with specified components such as the LED

board, LED detector intensity knob, printed circuit board (PCB), motor and batteries.

**CMAS software.** To enhance user experience and maintain true portability of the system, several software requirements were needed; these included:

- Wireless connection with the CMAS *via* Bluetooth;
- Real time display of the results;
- Internal data storage;
- Data connectivity to the Cloud, either *via* mobile network or WiFi.

A commonly available Android Tablet PC was used to implement these requirements (Samsung Galaxy Tab with 7-inch screen). The tablet runs Android Honey comb (v3.2) to provide Internet connectivity *via* a WiFi 802.11 a/b/g/n chip and has Bluetooth 3.0 connectivity, a GPS chip and a 3.0 MP rear camera. Data can be stored on an external SD card and the reported battery duration in normal use is 30 h. Data synchronisation with the Cloud can either happen on start up if an Internet connection is available, or if the user presses on the Cloud icon in the CMAS application. Among various remote hard drive services available, Dropbox (<http://www.dropbox.com>) was chosen since it allows easy data sharing with other users. Fig. 2A shows the CMAS with the Android tablet controller base station. See Fig. S2–S9, ESI† for more detail on the software and user interface.

**CMAS detection system.** The colorimetric detection and disc alignment systems are based on a low cost paired emitter detector diode (PEDD). The PEDD device consists of two 5 mm light emitting diodes, one serving as the light source and the other, in reverse bias mode, as the light detector (Fig. 2B).<sup>30,31</sup> The detector LED (660 nm) in output mode was firstly charged up to 5 V for 100  $\mu$ s and then switched to input mode. Light from the emitter LED (540 nm) generates a photocurrent in the reverse biased detector LED, resulting in discharge of the capacitance based voltage from an initial value of 5 V (logic 1) to a pre-set value of 1.7 V (logic 0). In order to provide a stable +5 V source to drive the circuit and LEDs, a voltage regulator running from a 9 V battery was employed. After passing through the microfluidic device, the observed light intensity is related to the discharge time of the acquired charge in the device.<sup>32</sup> The discharge time of the detector LED, thus the output signal, is dependent on the colour intensity of the solution.

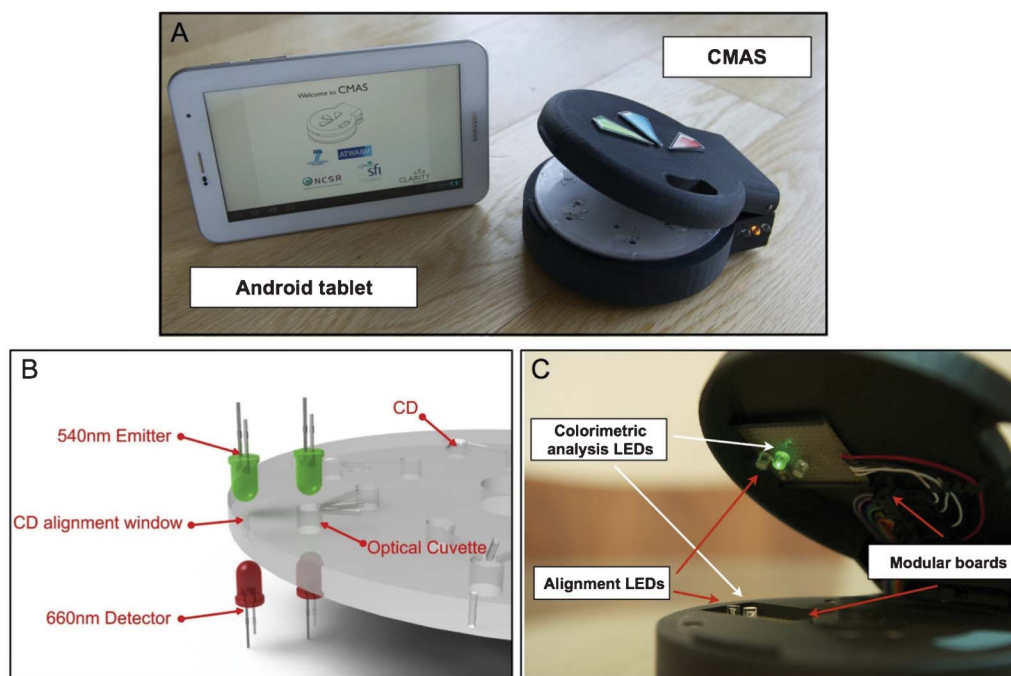


**Fig. 2** (A) Portable Android controller and CMAS, (B) schematic representation of the alignment/emitter/detector LEDs and (C) CMAS LED configuration specific to the nitrite CD (bottom right).

The alignment system is based on the second PEDD device and a CD alignment window fabricated in the CD adjacent to each microfluidic structure. The alignment of the optical cuvette with the respective PEDD detector (Fig. 2A) is achieved by the user manually when rotating the disc with the finger through the window in the top lid (Fig. 2C), using as a reference the alignment system explained above. Once the CD is correctly positioned (*i.e.*, the PEDD diodes are aligned with the CD alignment window, resulting in the lowest discharge time of the detector LED) a green light appears on the screen of the tablet. In order to optimise the sensitivity of the detector, the emitter LED intensity can be controlled by the potentiometer accessible on the side of the system (Fig. S1C, ESI†).

The analytical measurement is based on the following theoretical model which has been derived by Lau *et al.*<sup>33</sup>

$$\text{Log}(t) = \varepsilon Cl + \text{Log}(t_0)$$

where  $l$  is the optical path length through the solution (cm),  $\varepsilon$  the molar extinction coefficient,  $C$  the concentration of the absorbing species ( $\text{mol L}^{-1}$ ),  $t_0$  a constant that represents discharge time in the absence of the coloured species in solution ( $\mu\text{s}$ ) and  $t$  is the discharge time in the presence of the coloured species in solution ( $\mu\text{s}$ ). In the presented centrifugal disc the optical path length is 1.59 mm.

The emission spectrum of the emitter LED was obtained by using an Ocean Optics spectrometer (OOIBase 32 TM, Ocean Optics, Inc., Dunedin, USA).

### Experimental protocol for nitrite detection

In order to conduct a routine experiment on the CMAS, the operator simply needs to open the system and place the disc inside. The disc used for the analysis and the PEDD board have to match for the assay (in this case nitrite detection). After that, the water sample and the reagents are introduced (micropipetting) in the storage reservoirs of the disc (Fig. 3A).

Fluid distribution occurs *via* the centrifugal field generated through the spinning process (Fig. 3B). Rotation at 1000 rpm

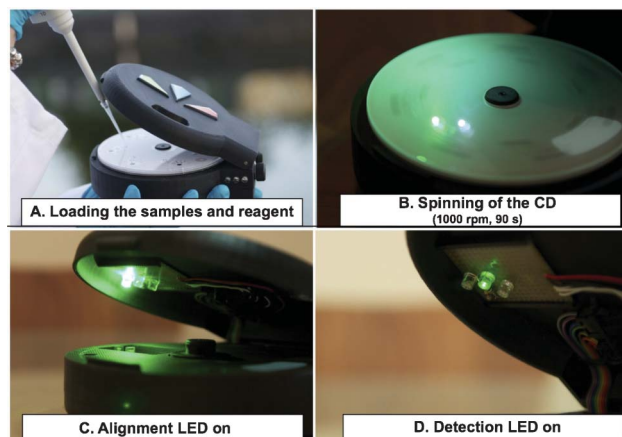


**Fig. 3** Photographs of CMAS during nitrite detection: (a) loading of freshwater samples, (b) spinning of the CD at 1000 rpm for 90 s, (c) on completion of spinning, the CD is manually aligned for PEDD detection (CMAS lid opened for clarity) and (d) PEDD detection (CMAS lid opened for clarity). A video of the system can be found at <http://tinyurl.com/dyoumds>.

for 90 s forces the liquids from the more central sample/reagent addition location outwards towards the detection chamber, where mixing (by diffusion) and the readout take place. The analysed freshwater samples were relatively clean, and therefore filtration of the sample prior to introduction into the microfluidic device was not necessary.<sup>29</sup> After stopping the CD and manual alignment of the LEDs (Fig. 3C), the intensity of the coloured solution, filling the detection chamber, was determined using the PEDD system of the CMAS (Fig. 3D). A video of the CMAS can be viewed at <http://tinyurl.com/dyoumds>.

### Repeatability measurements

The repeatability of the PEDD optical detector was determined by injecting a 1.0 mg L<sup>-1</sup> nitrite standard solution premixed with the Griess reagent to the same microfluidic structure followed by monitoring of the detector steady-state signal for 60 s (3 data points per second,  $n = 10$ ). After each measurement, the microfluidic structure was washed three times with DI water and dried with N<sub>2</sub>.

The repeatability of the measurements within one single CD was investigated by filling the seven microfluidic structures with an intensely coloured food dye solution (Goodall's, Ireland;  $\lambda_{\text{max}} = 505$  nm;  $n = 3$ ) and monitoring the detector steady-state signal for 60 s (3 data points per second;  $n = 3$ ).

Next, the difference in output signals across three separate centrifugal discs (CD1, CD2, CD3) was determined. One microfluidic structure on each CD was filled with the coloured food dye solution and the steady-state signal of the detector monitored for 60 s (3 data points per second;  $n = 3$ ). After each measurement, the microfluidic structure was washed three times with DI water and dried with N<sub>2</sub>.

### Nitrite assay calibration

Nitrite detection was carried out employing the Griess reaction method, which is based on the conversion of sulfanilic acid (Reagent A) to a diazonium salt by reaction with nitrite in acidic solution.<sup>34</sup> The diazonium salt is then coupled to *N*-(1-naphthyl)ethylenediamine (NED) (Reagent B), forming an azo dye, of which the intensity is directly related to nitrite concentration. The dye can be spectrophotometrically quantified/detected based on its absorbance at 547 nm (Fig. S10, ESI†). It was previously reported that the reagent volume which provided the most intense colour was determined as 0.2 : 3 (v/v) reagent to sample ratio and this was the ratio adopted throughout all the experiments.<sup>30</sup>

To demonstrate the utility of the system, a study of the colour formation between NO<sub>2</sub><sup>-</sup> and Griess reagent was performed using the CMAS and a commercially available UV-Vis spectrophotometer (Perkin-Elmer Lambda 900) as reference. The microfluidic colorimetric assay testing was carried out using various standard solutions containing a nitrite concentration from 0.0–1.2 mg L<sup>-1</sup>. The development of the nitrite Griess reagent complex colour intensity was monitored for 30 min. The sampling rate under this protocol was *ca.* 3 points per second.

### Analysis of freshwater samples

Freshwater samples were collected from five different inland waters in Ireland. The colorimetric reagent (2.1  $\mu$ L) and the filtered water sample (31.5  $\mu$ L) were loaded to the disc, and spun as previously described. Next, the solution was left to stand for 30 min for colorimetric development. The absorbance of the solution was measured at 540 nm using the PEDD system in CMAS and a UV-Vis spectrophotometer for reference (540 nm every 1 s for 30 min, cuvette = 1 cm). The resulting signal was measured continuously for 60 s. The sampling rate under this protocol was *ca.* 1 point per second.

## Results and discussion

CMAS presented several significant advances over the previously reported first generation system.<sup>29</sup> For example, spinning of the CD no longer has to be performed using a separate bench-top motor stand, which required manual transfer of the CD to the PEDD device for analytical measurements. In addition, sample testing had to be carried out in the dark to reduce the impact of ambient light noise, which affects the accuracy and precision of the measurements. Moreover, CMAS incorporates a stepper motor that allows fully integrated fluid manipulation and detection at point-of-need, and therefore enables true *in situ* water analysis (Fig. S11, ESI†).

### Centrifugal disc performance

The CD was designed, in this particular case, for water analysis in terms of nitrite *via* seven parallel microfluidics structures, allowing for sequential testing of multiple samples. Each of the microfluidic structures contained two inlet reservoirs for the uptake of the sample and the reagent, connected to a detection chamber ( $V_{\text{chamber}} = 34$   $\mu$ L) *via* the microchannels. These microchannels form a kind of capillary valve, which develops when the liquid encounters a transition from a small microchannel into a larger chamber. The burst frequency of the valve, *i.e.* the speed at which the surface tension force is overcome and the fluid continues to flow, was tested by spinning the disc at an increasing speed using increments of 2 rpm. The liquid movement to the detection chamber commenced in the region of *ca.* 250 rpm. A rotational speed of 1000 rpm was found to be sufficient to force the sample and the reagent towards the detection chamber, where mixing and detection occurred. Colour development was very rapid and kinetic measurements could be started in as little as 90 s for nitrite detection (see experimental protocol).

As previously reported,<sup>10</sup> the presence of bubbles in the detection chamber during analysis adversely affects the measured transmittance, and causes slightly degraded precision. Therefore an air vent, that connected with the detection chamber, was implemented, reducing substantially this problem and thereby improving the overall analytical performance (Fig. 1C).

### Centrifugal microfluidic analysis system

The portable device presented here provides many unique fluidic implementations for rapid and robust sample analysis. The system has been designed from the ground up specifically for integration with further downstream steps (e.g. automated alignment). The extremely compact footprint of the centrifugal disc provides extensive free space for integrating additional fluidics, in order to facilitate multi-parameter assays in future designs, e.g. nitrate, pH, turbidity, among others.

A unique function of CMAS is the modular PEDD alignment/detection configuration wherein the electronic boards, along with the PEDD devices, are easily interchangeable, thus allowing a wide range of centrifugal microfluidic layouts to be implemented using this system. Moreover, the modular board design can incorporate any low cost optical detector, including photodiodes, providing freedom of choice depending on the application. Another unique function of CMAS is that it allows for *in situ* universal colorimetric analysis for centrifugal platforms, since the light emitting diodes used as an optical detector cover a broad spectral range (LEDs in the spectral range *ca.* 247–1550 nm are commercially available).<sup>35,36</sup> At the same time, increased lifetime, low cost and reduced power consumption of the LEDs help keep the overall cost of the device low, making it more accessible for a broad range of potential applications.

The device supports any centrifugal disc design up to a thickness of 4.8 mm, which encompasses most of the centrifugal platforms presented in the literature. The motor enables rotational speed to be controlled over the range 500–4000 rpm. As previously reported,<sup>37</sup> the PEDD Device output can be continuously monitored during spinning of the disc at 0.5 Hz (30 rpm) and therefore the PEDD system is able to distinguish between chambers filled with solutions of different colours, during rotation. This implies that many samples can be analysed simultaneously during a single run, eliminating the need for start/stop detection, and manual alignment of the PEDD detector with the sample reservoir. Due to the wireless communication, method parameters can be controlled remotely and results can be downloaded in remote locations and displayed in real time. These capabilities, together with an adequate battery power supply (20 h of continuous operation) provide great flexibility for on-site water monitoring at remote locations.

### Optimisation of the PEDD parameters

The optimum wavelength ( $\lambda_{\max}$ ) to monitor the nitrite Griess reaction complex is in the range *ca.* 526–563 nm.<sup>38–41</sup> Under our experimental conditions (20.0  $\pm$  0.5 °C, NO<sub>2</sub><sup>−</sup> concentration range 0.2–1.2 mg L<sup>−1</sup>) we found the  $\lambda_{\max}$  to be 531 nm (Fig. S12, ESI†). Therefore, an emitter LED with a  $\lambda_{\max}$  of 525 nm (Fig. S13, ESI†) was employed as the light source, and a LED with a  $\lambda_{\max}$  660 nm that had a slightly smaller bandgap employed as the detector. The maximum absorbance of the nitrite Griess reaction complex therefore efficiently overlaps with the emission spectrum of the emitter green LED and will therefore allow high sensitivity.

### Repeatability of the PEDD measurements

The repeatability of the optical detector was determined by injecting a 1.0 mg L<sup>−1</sup> nitrite standard solution premixed with the Griess reagent as explained in the experimental section. An average discharge time was then calculated upon subtraction the output signal of blank (DI water). As shown in Fig. S14, ESI,† excellent repeatability was achieved with a relative standard deviation (RSD) of 0.24% between all measurements and an average signal (detector discharge time) of 12018  $\pm$  29  $\mu$ s ( $n = 10$ ). The raw data is presented in Table S1, ESI.†

### Repeatability of intra- and inter-centrifugal discs measurements

The average discharge times for the measurement of a coloured dye solution in seven microfluidic structures within one CD are presented in Fig. 4. Each value has been subtracted from the same average baseline generated with deionised water. The measurement of the coloured dye solution was repeated three times for each microfluidic structure with a RSD of typically *ca.* 1% or less for each structure. The raw data is presented in the Table S2, ESI.† The average discharge time of the coloured dye solution for the 21 runs for all the microfluidic structures was 16873  $\pm$  693  $\mu$ s (RSD = 4.11%). The results demonstrate that an event such as a colour variation can be measured using the PEDD within the CMAS (Fig. 4A) with reasonably good reproducibility, considering the fabrication of the structures within the discs is manual in nature. The expanded view of the graph shows that to a considerable extent, measurement variations within a disc are not random, but are consistently different from structure to structure (Fig. 4B). These inconsistencies in discharge times can be attributed to the manual fabrication of the CD's and exemplifies the fact that our results are strongly influenced by manual fabrication. Clearly, therefore, one can predict a substantial improvement in the platform performance will be achieved through adoption of automated techniques associated with mass production/manufacturing of the microfluidic structures.

Next, the repeatability experiments were carried out to compare the difference in output signals across three centrifugal discs (CD1, CD2, CD3) as explained in the experimental section. Each average value has been then subtracted from the same average baseline obtained with deionised water. The results are presented in Fig. 4C and the raw data can be found in Table S3, ESI.†

An average discharge time of 16858  $\pm$  8  $\mu$ s (RSD = 0.049%;  $n = 3$ ) was obtained for CD1, 16867  $\pm$  100  $\mu$ s (RSD = 0.59%,  $n = 3$ ) for CD2 and 16966  $\pm$  314  $\mu$ s (RSD = 1.85%,  $n = 3$ ) for CD3. This resulted in an average discharge time of 16897  $\pm$  173  $\mu$ s (RSD = 1.02%,  $n = 9$ ) for the detection of the dye solution using three separate CDs (fabricated manually). The results indicate that the CMAS measurements can be carried out using different centrifugal discs with very good repeatability. These results demonstrate that there is good within-disc and between-disc repeatability for the overall analytical approach based on the CMAS, despite the manual fabrication of the discs and microfluidic structures.

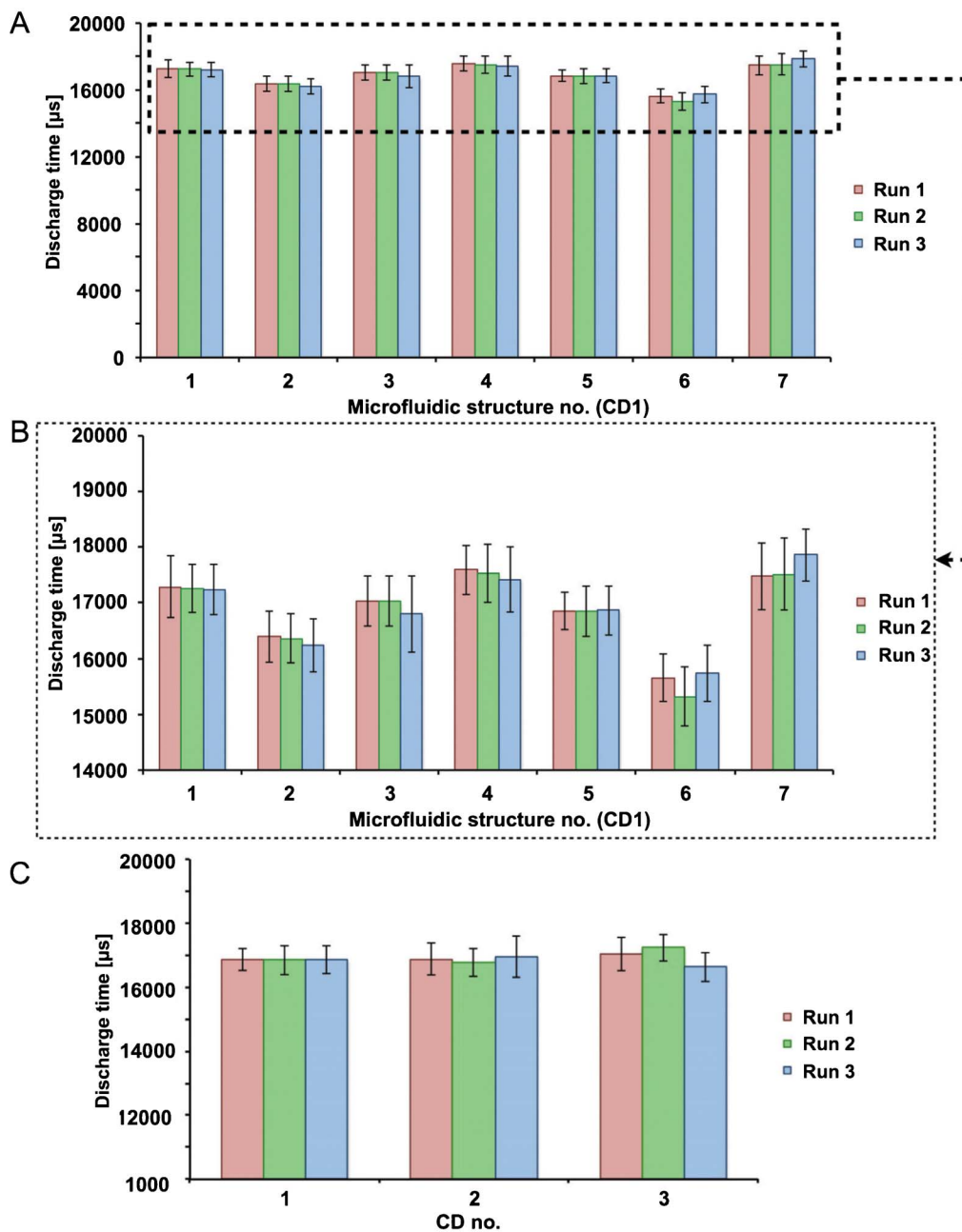


Fig. 4 (A) and (B) Repeatability of the microfluidic structures within a single CD and (C) between three separate CDs ( $n = 3$ ).

### CMAS sensitivity

To determine the limit of detection and limit of quantitation, we used the following approach. The LoD was estimated as three times standard deviation of blank response and LoQ was calculated as ten times standard deviation of blank response.<sup>42</sup> Based upon these formulations,<sup>42</sup> the LoD and LoQ for  $\text{NO}_2^-$  using the Greiss method on the CMAS platform were estimated to be  $9.31 \pm 0.09 \mu\text{g L}^{-1}$  and  $89 \pm 11 \mu\text{g L}^{-1}$  ( $n = 3$ ), respectively. As outlined in Table 1, these values are higher than the LoD and LoQ of the UV-Vis spectrophotometer ( $1.50 \pm 0.02 \mu\text{g L}^{-1}$  and  $14.8 \pm 0.2 \mu\text{g L}^{-1}$ , respectively). However, the CMAS platform is portable, can be operated at point of

**Table 1** A comparative summary of the data obtained for the detection of nitrite Griess reagent complex using both CMAS and a UV-Vis spectrophotometer ( $n = 3$ )

	CMAS ( $\lambda_{\text{max}} = 540 \text{ nm}$ )	UV-Vis spectrophotometer ( $\lambda_{\text{max}} = 540 \text{ nm}$ )
$R^2$	0.994	0.993
LoD	$9.31 \pm 0.09 \mu\text{g L}^{-1}$	$1.50 \pm 0.02 \mu\text{g L}^{-1}$
LoQ	$89 \pm 11 \mu\text{g L}^{-1}$	$14.8 \pm 0.2 \mu\text{g L}^{-1}$
RSD	1.02%	1.57%

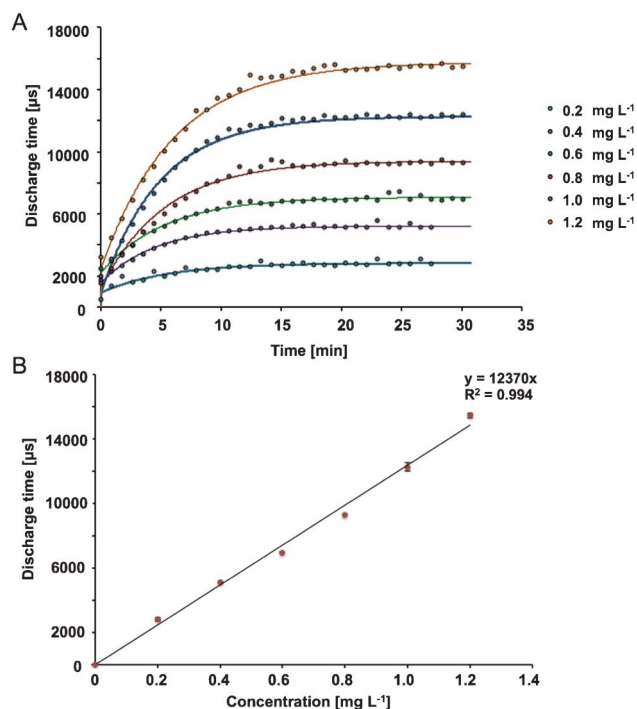


**Fig. 5** (A) Kinetic study of the colour formation between NO<sub>2</sub><sup>-</sup> and the Griess reagent at 540 nm (20.0 ± 0.5 °C), and fitted to the first order model and (B) discharge time versus nitrite Griess reagent complex concentration for the CMAS ( $n = 3$ ).

need, is relatively low cost to produce, and can process large numbers of samples *in situ* relatively quickly. Furthermore, the incorporation of wireless communications on CMAS means that data can be automatically transmitted to a remote cloud-based database. The CMAS demonstrates slightly higher value of coefficient of correlation ( $R^2 = 0.994$ ) than the UV-Vis spectrophotometer ( $R^2 = 0.993$ ) and an improved precision (RSD = 1.02%) in comparison to the results calculated from the bench top instrument (RSD = 1.57%), see Table 1.

The detection limits for nitrite achievable by this spectrometric standard procedures have been reported as typically being in the range 5–10 μg L<sup>-1</sup>, according to the World Health Organisation (WHO).<sup>43</sup> The detection limits achieved by CMAS fall into this region, which demonstrates the appropriate performance of the device. The results are particularly interesting because of the relatively small path length (1.59 mm), which according to the Beer-Lambert law has a

significant influence on transmittance measurement. Therefore, the results obtained with CMAS are useful not only for threshold testing, but also for both qualitative and quantitative measurements.

### Kinetics of colour development on the CMAS platform

The kinetics of the colour development for the detection of nitrite ion *via* the Griess method was monitored using six standard solutions 0.0–1.2 mg L<sup>-1</sup> of NaNO<sub>2</sub> using the CMAS (on-chip) at 540 nm for 30 min. This procedure was also performed using UV-Vis spectrophotometer (off-chip) by taking absorbance measurements over a similar time period per sample. Each standard solution was analysed in triplicate and the resulting kinetic curves for CMAS and UV-Vis spectrophotometer are presented in Fig. S15A and B, ESI†. From the graphs it is evident that the room temperature analysis yielded three reproducible kinetic curves for each standard solution. First-order kinetic models were fitted (Microsoft Excel Solver)<sup>44</sup> to each curve and the rate constants were calculated over the concentration range 0.0–1.2 mg L<sup>-1</sup> NO<sub>2</sub><sup>-</sup>. The average response and fitted models are presented in Fig. 5A for the CMAS and in the Fig. S16A, ESI† for the UV-Vis spectrophotometer. As shown in Table 2 and the Table S4A and B, ESI† the results obtained with the CMAS platform and the UV-Vis spectrophotometer are equivalent, with negligible difference, which further demonstrates similar performance of the portable CMAS platform, compared to a standard bench-top UV-Vis instrument.

### Calibration of the system for nitrite detection

The discharge time (detector signal) as a function of nitrite ion concentration is presented in Fig. 5B. The discharge time values for each concentration were calculated by subtracting the baseline signal obtained with deionised water from the discharge time value at steady state (an average of 50 data points was used; 3 data points per second) obtained with each standard. A  $R^2$  value of 0.994 (RSD: 1.45%) was calculated indicating a good linear response over the range 0–1.2 mg L<sup>-1</sup>. The calibration curve obtained with UV-VIS spectrophotometer is presented in Fig. S15B, ESI†. Absorbance values were calculated from an average of 17 data points (1 data point per second). Discharge times and absorbance values related to each NO<sub>2</sub><sup>-</sup> standard are presented in the ESI, Table S5A and B, ESI† respectively. The results demonstrate that the relative standard deviations for the three runs for each standard solution obtained with the CMAS platform are lower than those obtained with UV-Vis spectrophotometer (1.61% com-

**Table 2** Comparison of average rate constants obtained with the CMAS platform and the benchtop UV-Vis spectrophotometer for colour formation using NO<sub>2</sub><sup>-</sup> samples with the Griess method (20.0 ± 0.5 °C).

Sample no.	Nitrite concentration [mg L <sup>-1</sup> ]	CMAS average $k$ ( $n = 3$ ) ( $\times 10^{-3}$ )	UV-VIS average $k$ ( $n = 3$ ) ( $\times 10^{-3}$ )
1	0.2	1.03 ± 0.04	1.8 ± 0.2
2	0.4	1.27 ± 0.08	1.7 ± 0.3
3	0.6	1.09 ± 0.08	1.8 ± 0.2
4	0.8	1.04 ± 0.06	1.8 ± 0.2
5	1.0	1.2 ± 0.2	1.9 ± 0.4
6	1.2	1.0 ± 0.1	1.7 ± 0.3



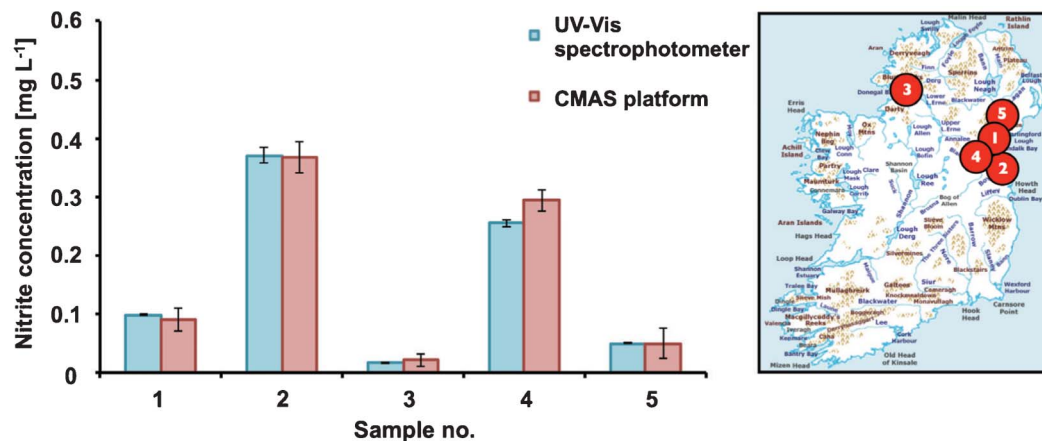


Fig. 6 Water nitrite analysis using a bench-top UV-Vis spectrophotometer (blue) and the CMAS (red) and a map of the sampling locations<sup>45</sup> ( $n = 3$ ).

pared to 2.96%). These results imply that the CMAS provided slightly more reproducible data compared to the UV-Vis bench-top instrument.

#### Nitrite detection in environmental water samples

Once the calibration method had been validated, the CMAS was then used to measure nitrite in freshwater samples from five different locations around Ireland. The concentration of nitrite ions measured using Griess reaction was reported within 30 min. As it is presented in Fig. 6 and Table S6, ESI,<sup>†</sup> the results obtained using the CMAS are within error to that of the UV-Vis spectrophotometer, which validate the utility of this device.

In comparison to the bench top microanalysis instrumentation based on the centrifugal platform presented by Salin *et al.*,<sup>10,12</sup> our technique provides comparable results of nitrite detection with a portability which in turn allows for on-site water analysis.

#### Practicality of the CMAS for on-site water analysis

It is worth discussing some of the practical implications and limitations of this system at this stage of its development. The disposables of the centrifugal platforms have been kept low cost, at <7 € per CD, translating to a low cost per test of only 1€; which could be further reduced in a mass-manufacturing setting. As discussed, operation of the system is simple, requiring only addition of the specimen and reagent, followed by software operation. Automation of the system translates to less user-introduced error and contamination, thus reducing the percentage of false positives. Furthermore, automation has obvious cost advantages in terms of reduction in labor. The cost of the CMAS in comparison to commercially available probes is relatively low; which can be reduced if mass production processes are used during fabrication. A cost breakdown of CMAS components is presented in Fig. S17, ESI.<sup>†</sup> The system presented is not a high-throughput system, but it is rapid and easy-to-use point of need device. As mentioned, the centrifugal platform has been designed to be part of a sample-to-answer system for water analysis, and not to replace larger, higher-throughput methods. While this system was

tested and validated using water samples, it should be noted that the CMAS has further potential applications beyond those of environmental monitoring, such as for the analysis of food samples for bacterial contamination and perhaps clinical diagnostics.

Infinity architectures can be constructed on centrifugal discs, which provide a great deal of versatility in developing dedicated assays for CMAS depending on the specific application. The size and architecture of the disc reservoirs govern the number of microfluidic units that can be placed on a single disc. Therefore, further miniaturisation and changes in the architectural design could easily allow for a greater number of assays per platform to be performed. While the case of nitrite ion detection is demonstrated as an example, clearly the platform can be readily adopted for the wide array of water parameters for which colorimetric methods exist, such as those presented by Hwang *et al.*<sup>13</sup> Future work will focus on the design of such architectures so that multiple analytes can be detected on a single disc, including pH and turbidity which were implemented within a centrifugal disc by our group before.<sup>29</sup>

## Conclusions

In addition to easy operation, robustness, the CMAS is a stand-alone, portable and compact device fully suitable for point-of-side analysis; it fulfils and indeed exceeds the requirements identified by Madou and co-workers.<sup>8</sup> Analysed parameters can be adjusted according to individual needs; results can be downloaded in remote locations and displayed in real time, and stored on web-databases for location independent access, which will make CMAS an ideal choice for many applications such as environmental or point-of-care diagnostics. The stand-alone capabilities of the system, combined with the portability and wireless communication, provide the flexibility needed for on-site monitoring, which in this example was nitrite detection in freshwater samples across Ireland. The LoD of CMAS ( $9.31 \pm 0.09 \mu\text{g L}^{-1}$ ) for nitrite is comparable to the detection limits

achievable by the spectrometric standard procedures and is within the range required for industrial and environmental applications. When compared to the UV-Vis spectrophotometer, the same value of coefficient of correlation ( $R^2 = 0.99$ ) was achieved with slightly improved RSD (1.02% compared to 1.57%), which indicates the good performance of CMAS. Due to all of the above-mentioned advantages, this system represents significant progress towards the realisation of truly stand-alone microfluidic platforms with the potential to change the way many important environmental and health related measurements are performed.

## Acknowledgements

The authors wish to thank to the Marie Curie Initial Training Network funded by the EC FP7 People Programme, Science Foundation of Ireland under grant 07/CE/I1147. K.J.F. acknowledges the European Commission for financial support through Marie Curie Actions International Reintegration Grant (IRG) (PIRG07-GA-2010-268365) and the Irish Research Council. This work has been supported by the Science Foundation Ireland under Grant No. 10/CE/B1821. MC thanks Mr. Brendan Heery for freshwater samples.

## References

- 1 K. R. Rogers, *Anal. Chim. Acta*, 2006, **568**, 222.
- 2 Hanna Instruments: [http://www.hannainst.com/usa/prods2.cfm?id=045001&ProdCode=HI\\_764](http://www.hannainst.com/usa/prods2.cfm?id=045001&ProdCode=HI_764) (accessed March 18, 2013).
- 3 API Test kits: <http://www.apifishcare.co.uk/product.php?sectionid=1&catid=4&subcatid=0&id=82> (accessed March 18, 2013).
- 4 Hach: [http://www.hachhydromet.com/web/ott\\_hach.nsf/id/pa\\_ds5-multiparameter-sonde.html](http://www.hachhydromet.com/web/ott_hach.nsf/id/pa_ds5-multiparameter-sonde.html). (accessed March 18, 2013).
- 5 YSI: <http://www.ysi.com/productsdetail.php?6920-V2-3> (accessed March 18, 2013).
- 6 M. Sequeira, D. Diamond, A. Daridon, J. Lichtenberg, S. Verpoorte and N. F. d. Rooij, *TrAC, Trends Anal. Chem.*, 2002, **21**, 816.
- 7 D. A. Duford, D. D. Peng and E. D. Salin, *Anal. Chem.*, 2009, **81**, 4581.
- 8 R. Gorkin, J. Park, J. Siegrist, M. Amasia, B. S. Lee, J.-M. Park, J. Kim, H. Kim, M. Madou and Y.-K. Cho, *Lab Chip*, 2010, **10**, 1758.
- 9 A. S. Watts, A. A. Urbas, E. Moschou, V. G. Gavalas, J. V. Zoval, M. Madou and L. G. Bachas, *Anal. Chem.*, 2007, **79**, 8046.
- 10 A. LaCroix-Fralish, J. Clare, C. D. Skinner and E. D. Salin, *CORD Conference Proceedings*, 2009, **80**, 670.
- 11 M. C. R. Kong and E. D. Salin, *Anal. Chem.*, 2012, **84**, 10038–10043.
- 12 X. Yongqing, E. J. Templeton and E. D. Salin, *Talanta*, 2010, **82**, 1612–1615.
- 13 H. Hwang, Y. Kim, J. Cho, J.-y. Lee, M.-S. Choi and Y.-K. Cho, *Anal. Chem.*, 2013, **85**, 2954.
- 14 D. Diamond, *Anal. Chem.*, 2004, **76**, 278A–286A.
- 15 B. S. Lee, J.-N. Lee, J.-M. Park, J.-G. Lee, S. Kim, Y.-K. Cho and C. Ko, *Lab Chip*, 2009, **9**, 1548.
- 16 G. T. Schembri, T. L. Burd, A. R. Kopf-Sill, L. R. Shea and R. Braynin, *J. Autom. Chem.*, 1995, **17**, 99.
- 17 M. Grumann, J. Steigert, L. Riegger, I. Moser, B. Enderle, K. Riebeseel, G. Urban, R. Zengerle and J. Ducee, *Biomed. Microdevices*, 2006, **8**, 1387.
- 18 J. Steigert, M. Grumann, M. Dube, W. Streule, L. Riegger, T. Brenner, P. Koltay, K. Mittmann, R. Zengerle and J. Ducee, *Sens. Actuators, A*, 2006, **130–131**, 228.
- 19 M. Grumann, L. Riegger, L. Pastewka, T. Brenner, R. Zengerle, J. Ducee, T. Nann, J. Riegler, O. Ehlert, K. Mittenbuhler and G. Urban, *Transducers 2005*, 5–9 June 2005, **2**, 1114.
- 20 N. Godino, R. Gorkin III, A. V. Linares, R. Burger and J. Ducee, *Lab Chip*, 2013, **13**, 685.
- 21 R. Gorkin III, C. E. Nwankire, J. Gaughran, X. Zhang, G. G. Donohoe, M. Rook, R. O'Kennedy and J. Ducee, *Lab Chip*, 2012, **12**, 2894.
- 22 M. J. Moorcroft, J. Davis and R. G. Compton, *Talanta*, 2001, **54**, 785–803.
- 23 J. Dutt and J. Davis, *J. Environ. Monit.*, 2002, **4**, 465–471.
- 24 R. A. Al-Okab and A. A. Syed, *Talanta*, 2007, **72**, 1239.
- 25 M. D. Patey, M. J. A. Rijkenberg, P. J. Statham, M. C. Stinchcombe, E. P. Achterberg and M. Mowlem, *TrAC, Trends Anal. Chem.*, 2008, **27**, 169.
- 26 Y. Xi, E. J. Templeton and E. D. Salin, *Talanta*, 2010, **82**, 1612.
- 27 K. S. Johnson and L. J. Coletti, *Deep-Sea Res., Part I*, 2002, **49**, 1291.
- 28 A. K. Hanson, *OCEANS 2000 MTS/IEEE Conference and Exhibition. Conference Proceedings (Cat. No.00CH37158)*, 2000, **3**, 1975.
- 29 M. Czugala, R. Gorkin III, T. Phelan, J. Gaughran, V. F. Curto, J. Ducee, D. Diamond and F. Benito-Lopez, *Lab Chip*, 2012, **12**, 5069.
- 30 M. O'Toole, R. Shepherd, K. T. Lau and D. Diamond, *Proc. SPIE-Int. Soc. Opt. Eng.*, 2007, **6755**, 67550P–1.
- 31 I. M. P. de Vargas-Sansalvador, C. Fay, T. Phelan, M. D. Fernandez-Ramos, L. F. Capitan-Vallvey, D. Diamond and F. Benito-Lopez, *Anal. Chim. Acta*, 2011, **699**, 216.
- 32 K. T. Lau, S. Baldwin, R. L. Shepherd, P. H. Dietz, W. S. Yezunis and D. Diamond, *Talanta*, 2004, **63**, 167.
- 33 K.-T. Lau, S. Baldwin, M. O'Toole, R. Shepherd, W. Yezunis, S. Izuo, S. Ueyama and D. Diamond, *Anal. Chim. Acta*, 2005, **557**, 111.
- 34 J. MacFaddin, Nitrate/nitrite reduction tests In: *Biochemical tests for identification of medical bacteria*, 3rd edn, Lippincott Williams & Wilkins, Philadelphia, 2000.
- 35 M. O'Toole and D. Diamond, *Sensors*, 2008, **8**, 2453.
- 36 A. Žukauskas, M. S. Shur and R. Gaska, *Introduction to Solid-State Lighting*, John Wiley & Sons, Inc., 2002.
- 37 R. Gorkin, M. Czugala, C. Rovira-Borras, J. Ducee, D. Diamond and F. Benito-Lopez, *Solid-State Sensors, Actuators and Microsystems Conference (Transducers)*, Beijing, China, 2011, p. 2526.
- 38 P. C. Hauser, T. W. T. Rupasinghe and N. E. Cates, *Talanta*, 1995, **42**, 605.
- 39 F. R. P. Rocha and B. F. Reis, *Anal. Chim. Acta*, 2000, **409**, 227.

- 40 W. Frenzel, J. Schulz-Brussel and B. Zinvirt, *Talanta*, 2004, **64**, 278.
- 41 E. T. Steimle, E. A. Kaltenbacher and R. H. Byrne, *Mar. Chem.*, 2002, **77**, 255.
- 42 A. Shrivastava and V. Gupta, *Chron. Young Sci.*, 2011, **2**, 21–25.
- 43 World Health Organization, *Guidelines for drinking-water quality [electronic resource]: incorporating 1st and 2nd addenda*, vol. 1, Recommendations, Geneva, 2008.
- 44 D. Diamond and V. C. A. Hanratty, *Spreadsheet Applications for Chemistry Using Microsoft Excel*, John Wiley and Sons, New York, 1997.
- 45 [http://en.wikipedia.org/wiki/File:Ireland\\_physical\\_large.png](http://en.wikipedia.org/wiki/File:Ireland_physical_large.png) (accessed April 14, 2012).